J. of Thermal Science Vol.13, No.1

Flow-Field of an Axisymmetric Lobed Mixer

L.Y. Jiang I. Yimer S. Manipurath I. Campbell W.E. Carscallen
Gas Turbine Environmental Research Centre, Aerodynamics Lab, Institute for Aerospace Research, National Research Council Canada, 1200 Montreal Road, Ottawa, Ontario, Canada, K1A 0R6, Tel. 613-993-9235, E-mail: leiyong.jiang@nrc-cnrc.gc.ca

The flow-field of a fuel/air mixing system with an axisymmetric lobed mixer was numerically investigated. Large-scale streamwise vortices are formed immediately downstream of the mixer trailing edge, stretched further downstream, and finally broken into fragments where more intense mixing occurs. Both numerical and experimental results indicate that the length required for streamwise vortices breakdown in the confined flow-field of an axisymmetric lobed mixer is much shorter than that in the case of planar lobed mixers subject to parallel freestreams. For the conditions studied, the streamwise vortices start to breakdown at three wavelengths downstream of the mixer trailing edge.

Keywords: axisymmetric lobed mixer, confined flow, fuel/air mixing.

Introduction

Lobed mixers have been applied to a number of engineering applications, such as jet noise reduction, infrared suppression and improvement of propulsion efficiency for gas turbine engines. More recently, they have emerged as an attractive method for enhancing fuel/air mixing in advanced combustion systems to reduce pollutant formation and to improve efficiency.

The underlying physics of planar lobed mixers in parallel freestreams has been extensively studied by a number of researchers[1~8]. They have pointed out that the counter-rotating pairs of streamwise vortices generated by the lobed mixer play a key role in mixing enhancement, where the interfacial surface area between two streams and the local gradients of flow properties are increased. Werle et al.[1] found that the streamwise vortices experience a three-step process, i.e., formation, intensification and breakdown, and more intense mixing occurs in the third region. Eckerle et al.[3] confirmed the above observation and pointed out that the length required for the flow to reach the third step was a function of the velocity ratio across the mixer. The evolution of streamwise vortices was further studied by Yu[9] in a low-speed wind tunnel at a freestream velocity ratio of 1:1. It was found that there was no vortex breakdown within seven wavelengths downstream of the mixer trailing edge for three trailing edge configurations tested.

In addition to the large-scale streamwise vortices, vorticity components or transverse vortices parallel to the trailing edge are also present in the flow-field when the freestream velocities on either side of the lobe are not equal. These relatively small-scale transverse vortices associated with the instability of the shear layers between the two streams can further intensify the mixing process[4,5]. Moreover, there are also horseshoe vortices formed around the front of the lobes. However, the strength of these vortices is an order of magnitude less than either streamwise or transverse vortices and has little impact on the overall mixing process[8].

Lobed mixers with geometrical configurations similar to the turbofan engine exhaust section were intensively studied in 1970s and 1980s. To date, it is still an active research subject aiming at design optimisation of lobed mixers or ejectors to improve engine performance and noise reduction[10,11]. Among the significant findings of these studies is that the lobed mixer can generate streamwise vortices more efficiently (i.e., less pressure drop) than the conventional methods[12].

In contrast, studies of lobed mixers relevant to practical combustion systems are rare. With flow visualisation of a passive scalar, Belovich et al.[12] explored the mixing enhancement of three lobed mixers in an axisymmetric coaxial jet. Recently, Hu et al.[13]

Received 2003

measured instantaneous and averaged velocities and inferred vorticity maps in an axisymmetric lobed jet flow with a 3-D PIV system. However, these investigations were carried out in open flows where the conditions are benign to advanced laser diagnostics.

In this paper, the confined flow-field of an axisymmetric 12-lobe convoluted mixer is numerically studied. The geometrical set-up of the mixing system is pertinent to many combustion systems using advanced lean premixing concepts and gaseous fuels[14]. The objective of the present work is to understand the flow features and mixing augmentation mechanisms of the lobed mixer in axisymmetric confined flows. The numerical results are compared with the limited experimental results obtained from a 2-D PIV system.

Numerical Simulation

Experimental measurement

Fig.1 schematically shows a portion of the experimental set-up used for the fuel/air mixing research at the Gas Turbine Environmental Research Centre (GTERC). More detailed information of the experimental facility and instrumentation are available in reference [14]. The mixer/fuel spoke section, immediately downstream of the contraction section of the inlet flow-conditioning chamber, is 177.8 mm long and 50.8 mm in diameter. It hosts a 12-lobe convoluted mixer attached to the enlarged section of the central fuel pipe. The lobed mixer has a wavelength (λ) of 9.69 mm, lobe height (h) of 14.5 mm and wall thickness of 1 mm. The inward and outward penetration angles (α) are 22.6° following a 15 mm long straight splitter. There are six fuel spokes welded to the enlarged end of the fuel pipe and the outside diameter of spokes is 3.175 mm. Since the objective of the present work is to study the flow features and the fuel volume flow rate is only a few percent of that of air, the fuel flow was neglected in the numerical simulation and turned off in the PIV measurement.

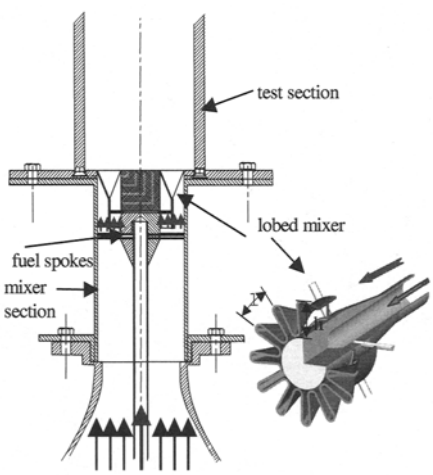

Fig.1 Schematic of the experimental set-up

Downstream of the mixer/fuel spoke section is the test section. It is 381 mm long, and has a square cross-section of 52×52 mm and a 50.8 mm circular exit at the downstream end. The corners of the cross-section are rounded with a radius of 10.2 mm. An exhaust chamber is connected to the test section exit and the flow is drawn out by an extraction fan.

PIV velocity measurements were carried out at an airflow rate of 1580 SLPM. The corresponding Reynolds number was 3.8×10^4 based on the mixer diameter and 7.6×10^3 according to the wavelength of the lobed mixer. Double-pulsed laser generated by twin Nd:YAG lasers from New Wave Corp. was used to form a light sheet through the test section. To achieve this, an optical transmission set-up was arranged and the resultant thickness of the laser sheet was about 1 mm. A high resolution CCD camera with 1280×1024 pixels (FLOWMASTER3 from La Vision) was aligned orthogonal to the laser sheet and a narrow-band filter at 532 nm was mounted in front of a collection lens to minimise background noise. To synchronise operations of the camera and laser, a programmable timing unit was employed. A time interval of 6~15 μs between pulsed laser pairs was used to provide an average pixel displacement of 2. The region of interest covered a quadrant of the test cross-section with a camera resolution of 0.027 mm/pixel. Al_2O_3 particles with a nominal size of ~1 μm were used to seed the flow. Image acquisition and image processing were all done by a PC equipped with the LaVision system. Two-dimensional velocity vectors were then calculated using the second-order standard cross-correlation and an adaptive window shifting with a final interrogation window size of 16×16 pixels. At a given cross-section, sixty instantaneous image pairs were taken at a frequency of 4 Hz to provide the mean flow field.

Computational domain

The computational domain covered the mixer/fuel spoke section and the test section. Fig.2 shows the middle portion of these two sections. One quarter of the flow-field was considered due to the symmetry in geometry and a hybrid hexahedral/tetrahedral mesh was generated over the whole computational domain. Fig.3 shows the mesh of the top portion of the mixer/fuel spoke section. To resolve the flow details, fine meshes were generated around the lobed mixer, fuel spokes and the upstream portion of the test section. Hex or prism layers were generated at all wall boundaries to properly account for the wall boundary effect and the Y plus values were maintained in a range from 1 to 5. Volume mesh adaption was performed to reduce rapid variation of cell volumes and to improve numerical accuracy and

convergence speed. The total number of cells was 1.66 million. Another mesh was also created using both velocity gradient and volume adaption to check grid independence of the numerical solutions, and the total cells reached 2.05 million. The difference in numerical solutions obtained from these two meshes was negligibly small.

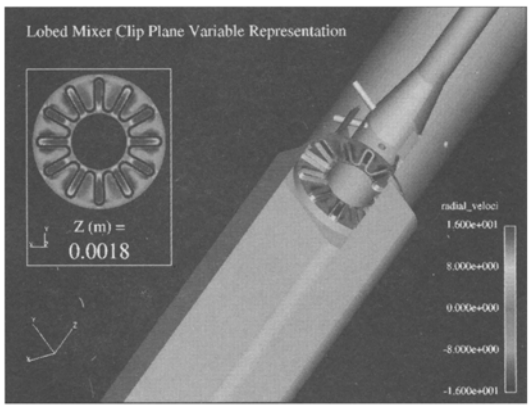

Fig.2 The middle portion of the computational domain

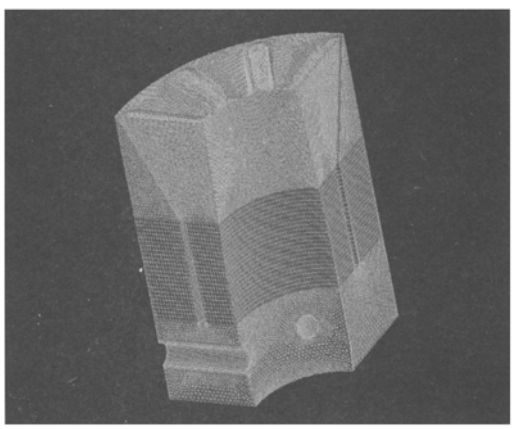

Fig.3 Mesh of the top portion of the mixer/fuel spoke section

Boundary conditions and physical models

The PIV measured velocity profile and turbulence intensity were imposed at the air inlet of the mixer/fuel spoke section. The discrepancy of the airflow rate calculated from the velocity profile was less than 2% in comparison with the metered value. A hydraulic diameter of 38.1 mm and a room temperature of 293 K were also assigned at the air inlet. At the exit of the test section, atmospheric pressure was defined.

The re-normalisation group (RNG) k-ε turbulence model was used to model turbulence in the flow. It is considered that the model is capable of accounting for the effects of flow swirling and rapid straining and has shown substantial improvements over the standard k-ε model, where the flow features include strong stream-wise curvature, vortices, and rotation[15,16]. For the wall boundaries, an enhanced wall boundary treatment was applied, where the traditional two-layer zonal model is enhanced by smoothly blending the viscous sub-layer and fully turbulent regions.

Solution method

A segregated solver of a commercial software package, Fluent, was used to resolve the flow-field with the second-order accuracy scheme. The normalised residual was less than 1.7×10^{-5} for velocity components, and 5×10^{-5} for turbulent kinetic energy and dissipation rate. For the continuity equation, the residual reached 8×10^{-4} normalised by the largest absolute residual in the first five iterations. The computations were performed on a dual, 1 GHz Pentium III processor unit with 2GB of RAM memory.

Numerical Results

Flow patterns and velocity contours

Fig.4 illustrates the variation of axial velocities along the axis of symmetry downstream of the mixer trailing edge at cross-sections z/λ=0.2 to 4. Two recirculation zones (negative axial velocities) are observed due to the sudden expansion of the flow passage. One is behind the bluff body of the fuel supply in the centre region of the flow-field and the other is at the corner of the square cross-section of the test section (see Figs.1,2). The magnitude and gradient of the axial velocity decrease rapidly downstream of the mixer due to the enhanced turbulent mixing. Fig.5 shows the contours of radial velocities at the same cross-sections as in Fig.4. Note that at z/λ=0.2 and 1, large outward (positive) radial velocities occur in the outward lobe regions, while large inward (negative) radial velocities are observed in the inward lobe regions. Flow moving in the opposite directions forced by the convoluted mixer generates large-scale streamwsie vortices and greatly enhances the mixing process. As in the case of axial velocity, the

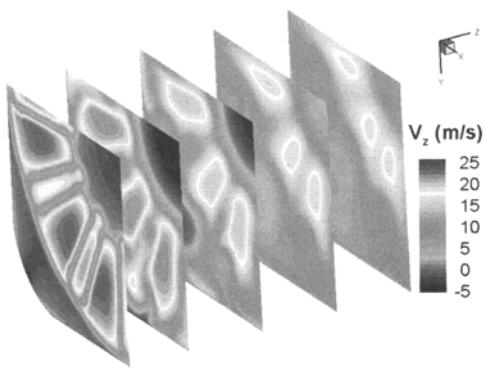

Fig.4 Axial velocity distributions at z/λ = 0.2, 1, 2, 3 and 4

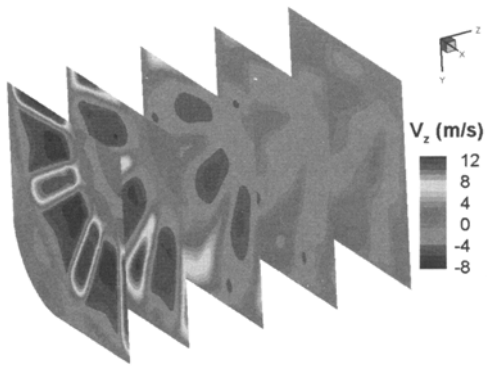

Fig.5 Radial velocity distributions at $z/\lambda = 0.2$, 1, 2, 3 and 4

radial velocity magnitude and gradient decrease rapidly away from the mixer trailing edge.

Streamwise Vortex Development

Fig.6(a) shows the velocity vectors at the cross-section, z/λ=0.2. Flow motions towards and away from the centre of symmetry are clearly observed in the inward and outward lobe regions, respectively. Fig.6(b) presents a vorticity contour plot of the resulting streamwise vortices at the same cross-section. Superimposed on the vorticity plot is the trailing edge contour of the lobed mixer. Three counter-rotating pairs of ribbon vortices are formed immediately downstream of the mixer trailing edge. Note that the magnitudes of these vortices are large and their gradients are steep. In addition to streamwise vortices, counter-rotating pairs of horseshoe vortices wrapping around each inward and outward lobe peaks are also predicted. In the present study, transverse vortices are not considered since the upstream flow velocity is the same on either side of the mixer and the effect of these vortices on the flow-field is believed insignificant [4,5,8].

Fig.7 gives the vector and streamwise vorticity plots at z/λ=1.5, the six ribbon vortices become wider and distorted. As expected, a pair of counter-rotating vortices is formed at the corner of the test section due to the corner effect. Further downstream of the mixer, as shown in Figs.8(a) and (b) for section z/λ=3.0, the six vortices are starting to breakdown into fragments, and the flow-field becomes much more complicated than that in the case of planar lobed mixers subject to parallel co-flowing freestreams. The pair of corner vortices becomes stronger at this cross-section.

Figs.6~8 illustrate the formation, stretch/expansion,

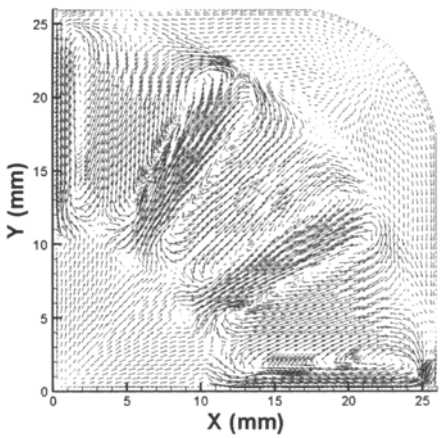

Fig.6(a) Vector plot at $z/\lambda = 0.2$

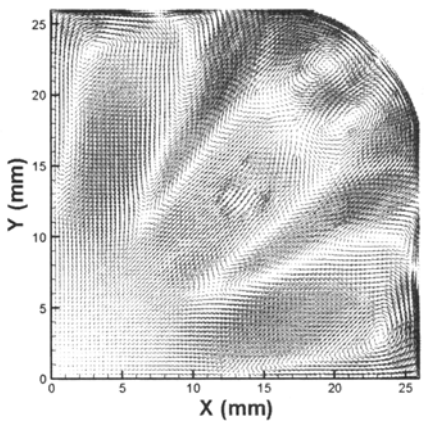

Fig.7(a) Vector plot at $z/\lambda = 1.5$

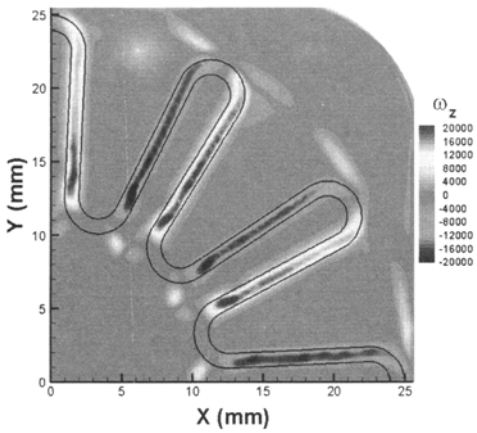

Fig.6(b) Streamwise vorticity at $z/\lambda = 0.2$

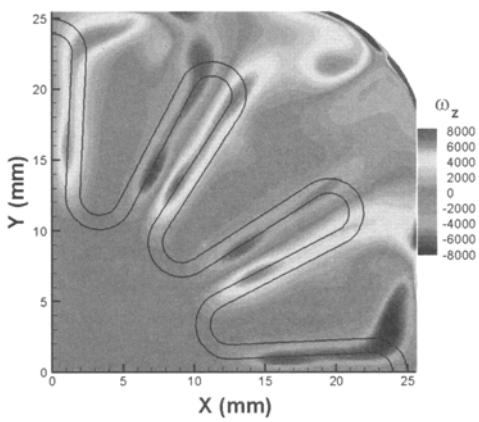

Fig.7(b) Streamwise vorticity at $z/\lambda = 1.5$

and breakdown of streamwise vortices generated by the 12-lobe convoluted mixer. As mentioned earlier, Yu[9] studied the development of streamwise vortices of three types of planar lobed mixers in a low-speed wind tunnel, where the lobe wavelength and lobe height were 33 mm, the penetration angle was 22° and a freestream velocity ratio was one. He found that no vortex breakdown was observed within seven wavelengths downstream of the mixer trailing edge for the three configurations. One of the important findings from the present study is that the breakdown of the streamwise vortices in the confined flow-field of an axisymmetric lobed mixer is much earlier than those observed in planar lobed mixers. This information is important for design of mixing ducts to ultimately reduce combustor length.

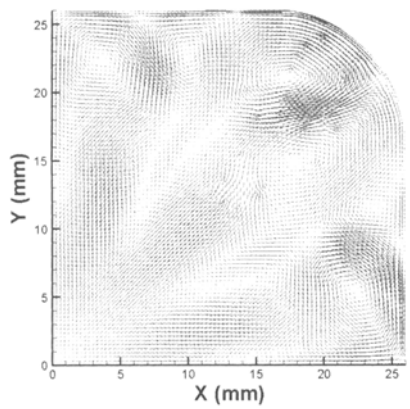

Fig.8(a) Vector plot at $z/\lambda = 3.0$

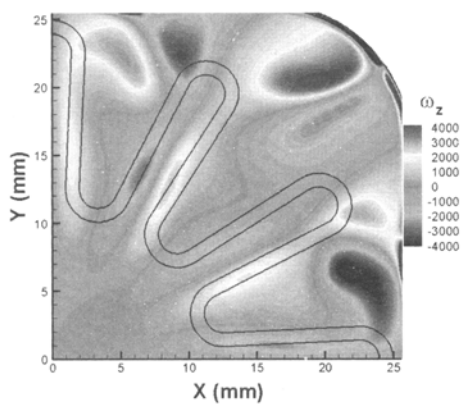

Fig.8(b) Streamwise vorticity at $z/\lambda = 3.0$

Comparison with Experimental Results

The velocity distributions at a number of horizontal cross-sections were measured by the PIV system and the streamwise vorticity distributions were inferred. Figs.9~11 show the streamwise vorticity contours at cross-sections z/λ=0.8, 1.5 and 3.0 with a view window of 20.5×21.5 mm. Similar to the numerical results, the strength of vortices decreases with an increase in distance downstream of the lobed mixer trailing edge. Three counter-rotating pairs of streamwise vortices are clearly observed at sections z/λ=0.8 and 1.5. At section, z/λ=3.0, the counter-rotating vortices are starting to intersect with each other and their shapes are not well defined, which implies the vortex breakdown occurs. This is in consistent with the numerical observations. Like the numerical simulation, a pair of counter-rotating vortices is also observed at the corner of the square cross-section for z/λ=0.8, 1.5 and 3.0, and the strength increases with an increase in downstream distance.

It is noted that the vorticity magnitudes of the numerical results are higher than the corresponding experimental values (Figs.7,8,10,11). Difference in spatial resolution, deficiencies of numerical physical models and measurement uncertainties may contribute to this discrepancy. To some extent, averaging over and between the interrogation windows was assumed in the PIV measurement, which tended to smooth gradients of flow properties. Deficiencies of the current turbulence models were observed in the previous combustor simulation[16]. It should be mentioned that the direct comparison of vorticity between experimental and numerical results regarding lobed mixers has never seen before in authors' knowledge. Besides, another

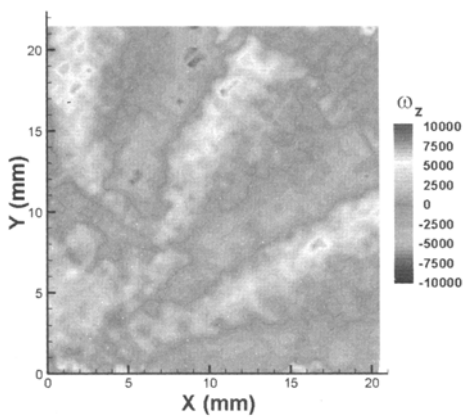

Fig.9 Streamwise vorticity at $z/\lambda = 0.8$

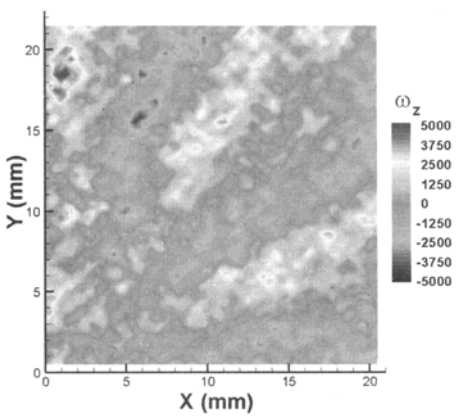

Fig.10 Streamwise vorticity at $z/\lambda = 1.5$

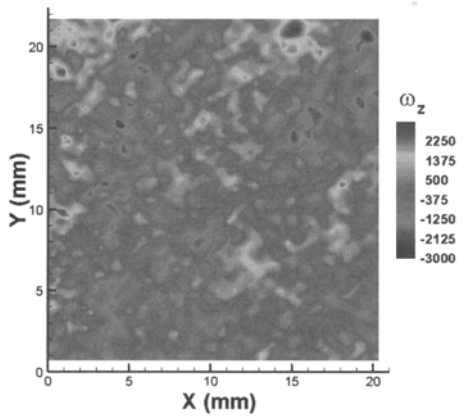

Fig.11 Streamwise vorticity at $z/\lambda = 3.0$

discrepancy between the prediction and measurements is the flow rotation in the central recirculation zone. This is experimentally observed (Figs.9~11), however it is not shown in the numerical results (Figs.7,8). It is well known that the flow in the recirculation zone is highly unsteady. In the numerical simulation, the mean velocity averaged over an infinite time was implied, while in the PIV measurements, only sixty instantaneous images were assembled. Further investigation regarding these discrepancies will be addressed in the future.

Summary

The confined flow-field of an axisymmetric lobed mixer in a fuel/air mixing system relevant to practical low emission combustion designs was simulated. The numerical solutions were qualitatively compared with the PIV experimental results. The streamwise vortices experience a three-step process, i.e., formation, stretch and breakdown. This process in the confined flow of the axisymmetric lobed mixer is significantly accelerated. For the test configuration and conditions, the streamwise vortices start to breakdown three wavelengths downstream of the mixer trailing edge, which agrees with the experimental measurements.

References

[1] Werle, M J, Paterson, R W, Presz, W M Jr. Flow Structure in a Periodic Axial Vortex Array. AIAA paper 87-0610, 1987

[2] Barber, T, Paterson, R W, Skebe, S A. Turbofan Forced Mixer Lobe Flow Modelling, Part I, Experimental and Analytical Assessment. NASA CR 4147, 1988

[3] Eckerle, W A, Sheibani, H, Awad, J. Experimental Measurement of the Vortex Development Downstream of a Lobed Forced Mixer. American Society of Mechanical Engineers, paper 90-GT-27, 1990

[4] Manning, T A. Experimental Studies of Mixing Flows with Streamwise Vorticity. [M.S. Thesis]. Massachusetts Institute of Technology, Cambridge, MA, 1991

[5] McCormick, D C, Bennett, J C Jr. Vortical and Turbulent Structure of a Lobed Forced Mixer Free-Shear Layer. AIAA paper 93-0219, 1993

[6] Yu, S C M, Yeo, J H, Teh, J K L. Velocity Measurements Downstream of a Lobed-Forced Mixer with Different Trailing-Edge Configurations. Journal of Propulsion and Power, 1995, 11(1): 87—97

[7] O'Sullivan, M N, Krasnodebski, J K, Waitz, I A, et al. Computational Study of Viscous Effects on Lobed Mixer Flow Features and Performance. Journal of Propulsion and Power, 1996, 12(3): 449—450

[8] Waitz, I A, Qiu, Y J, Manning, T A, et al. Enhanced Mixing with Streamwise Vorticity. Prog. Aerospace Sci., 1997, 33: 323—351

[9] Yu, S C M. Some Aspects of the Flows Behind Lobed Forced Mixers. International Communication in Heat Transfer, 1994, 21(6): 849—858

[10] Koutmos, P, McGuirk, J J. CFD Predictions of Lobed Mixer Performance. Computer Methods in Applied Mechanics and Engineering, 1995, 122: 131—144

[11] Nakamura, Y, Oishi, T. Research and Development of Mixer-Ejector Nozzle. Proceedings of the International Gas Turbines Congress, Indianapolis, U.S.A., 1999. 219—224

[12] Belovich, V M, Samimy, M, Reeder, M F. Dual Stream Axisymmetric Mixing in the Presence of Axial Vorticity. Journal of Propulsion and Power, 1996, 12(1)

[13] Hu, H, Saga, T, Kobayashi, T, et al. Mixing Process in a Lobed Jet Flow. AIAA Journal, 2002, 40(7)

[14] Yimer, I, Campbell, I. Parametric Study to Optimise Air/Fuel Mixing for Lean, Premix Combustion Systems. Proceedings of 2002 International Joint Power Generation Conference, Amsterdam, 2002. IJPGC2002-26086

[15] Yakhot, V, Orszag, S A. Re-normalisation Group Analysis of Turbulence: I. Basic Theory. Journal of Scientific Computing, 1986, 1(1): 1—51

[16] Jiang, L Y. Campbell, I, Yimer, I. Numerical Simulation of a Generic Combustor. AIAA paper 2002-1089, 2002